Geomechanics and Engineering, *Vol. 33, No. 2 (2023) 203-209*
https://doi.org/10.12989/gae.2023.33.2.203

Subsurface anomaly detection utilizing synthetic GPR images and deep learning model

Ahmad Abdelmawla, Shihan Ma, Jidong J. Yang and S. Sonny Kim*

University of Georgia (College of Engineering, School of Environmental, Civil, Agricultural and Mechanical Engineering, 597 DW Brooks Drive Athens, GA 30602, USA

(*Received November 28, 2022, Revised March 3, 2023, Accepted April 7, 2023*)

Abstract. One major advantage of ground penetrating radar (GPR) over other field test methods is its ability to obtain subsurface images of roads in an efficient and non-intrusive manner. Not only can the strata of pavement structure be retrieved from the GPR scan images, but also various irregularities, such as cracks and internal cavities. This article introduces a deep learning-based approach, focusing on detecting subsurface cracks by recognizing their distinctive hyperbolic signatures in the GPR scan images. Given the limited road sections that contain target features, two data augmentation methods, i.e., feature insertion and generation, are implemented, resulting in 9,174 GPR scan images. One of the most popular real-time object detection models, You Only Learn One Representation (YOLOR), is trained for detecting the target features for two types of subsurface cracks: bottom cracks and full cracks from the GPR scan images. The former represents partial cracks initiated from the bottom of the asphalt layer or base layers, while the latter includes extended cracks that penetrate these layers. Our experiments show the test average precisions of 0.769, 0.803 and 0.735 for all cracks, bottom cracks, and full cracks, respectively. This demonstrates the practicality of deep learning-based methods in detecting subsurface cracks from GPR scan images.

Keywords: data augmentation; deep learning; ground penetrating radar; object detection; pavement inspection

1. Introduction

Cracks are one of the major distresses in pavement, largely arising from material irregularities and internal stresses, coupled with dynamic traffic loadings and weather effects. Their presence indicates impaired structural integrity that often leads to faster deterioration of pavement. The internal cracks within a pavement are often initialized from the bottom of the asphalt layer or the base layers, generally referred to as bottom-up cracks. These cracks are attributable to tensile stress at the bottom of these layers due to the surface wheel loads or weather-induced effects. Given the hidden nature of these internal defects, proper detection and assessment of these cracks are extremely helpful in diagnosing the damages and causes, and selecting the appropriate repair or rehabilitation countermeasures.

Ground Penetration Radar (GPR) is a popular non-destructive technology and has been used to identify subsurface anomalies, such as pipes, rebars, and internal cavities. Recent GPR systems equipped with air-coupled antennas have been mounted on vehicles to enable convenient inspection of pavement subsurface conditions at highway speeds (Saarenketo and Scullion 2000, Bendetto and Pensa 2007, Abdelmawla and Kim 2020). This modern practice has resulted in tremendous GPR scan data, which becomes impossible to analyze manually.

*Corresponding author, Dr.
E-mail: kims@uga.edu

http://www.techno-press.org/?journal=gae&subpage=7
ISSN: 2005-307X (Print), 2092-6219 (Online)

Automated subsurface anomaly detection algorithms become necessary to handle this task in practice.

The research by Sudyka *et al*. (2018) showed practicality of characterizing pavement cracking process. Their method allows to examine the structure of the cracks and assess the depth of their roots as well as diagnosing structural integrity in more complex situations than simple transverse crack fracture. Beside the surface-initiated cracks, it is practically useful to analyze the cracks that are initiated from the bottoms of pavement layers that may or may not have propagated to the surface yet.

According to Diamanti *et al*. (2010), vertical crack responses could be observed in pavement, with or without visible surface cracks. These cracks could be noticed as reflected cracks at joints in pavements under an asphalt overlay or as cracks propagated from underneath granular materials due to localized water infiltration.

The GPR measurements are traditionally evaluated by experienced survey personnel to detect the position and size of some target objects (Nuaimy *et al*. 2000, Gamba and Lossani 2000). To overcome the problems associated with human inspection methods, Neural networks (NN) were developed for automatic recognition of targets' features in GPR images (Nuaimy *et al*. 2000, Gamba and Lossani 2000). The frequency characterization of the GPR images was employed for feature detection by NN as mentioned in Nuaimy *et al*. (2000), while the spatial signatures of the GPR images were used after binary encoding with a threshold according to Gamba and Lossani (2000). These studies have shown the effectiveness of NNs in the feature recognition task with GPR images. However, NN-based

methods lack the generalization capability for recognizing complex features. Furthermore, accurate target identification requires an ideal noise state and appropriate preprocessing (e.g., clutter removal), assumptions of which sometimes fail.

Deep convolutional neural networks (CNNs) have recently been used in pattern recognition (Girshick *et al.* 2014, Ding *et al*. 2016) and classification (Krizhevsky *et al*. 2012, Chen *et al.* 2016). Compared to traditional NN, Deep CNNs feature shared local filters to enable location-invariant feature extraction at various levels. The higher-level features are composable from the lower-level features, leading to hierarchical feature representation for complex pattern recognition tasks. This paper proposes to train a popular real-time object detection model, YOLOR (You Only Learn One Representation), initially developed by Wang *et al.* (2021), for pavement subsurface crack detection. To deal with the scarcity of target data (i.e., subsurface cracks), two novel data augmentation methods, i.e., target feature insertion and generation, are employed to generate a relatively large dataset for YOLOR model training. The paper is organized in five sections. The YOLOR model is first introduced in Section 2. The data acquisition and augmentation are then presented in Section 3. Our experiments and results are discussed in Section 4, followed by conclusions in Section 5.

2. YOLOR

YOLOR is one of the most popular real-time object detection algorithms, famous for its speed and accuracy. It has been used in various object detection applications. In YOLOR, a unified network is proposed to encode both explicit knowledge and implicit knowledge, which emulates the function of the human brain that can learn knowledge from normal learning as well as subconsciousness learning. The unified network aims to integrate implicit knowledge and explicit knowledge to enable general representation that can be utilized for various tasks. By introducing implicit knowledge in object detection, YOLOR achieves an accuracy comparable to YOLOv4, but with significantly reduced inference time. This places YOLOR one of the best real-time object detection algorithms.

In this study, a YOLOR model is trained to detect two classes of subsurface cracks: bottom cracks and full cracks. To leverage transfer learning, the network is initialized with COCO-pretrained weights and finetuned with our GPR scan image dataset.

3. Data acquisition and augmentation

The GPR scan images are collected from various road sections in Atlanta and Athens, Georgia, USA using the University of Georgia (UGA)'s GPR van (see Fig. 1), where the antennae are mounted at the back of the van.

With over 400 miles of road scan, the obtained GPR image data are abundant. But the target features are scarce in the retrieved image data to successfully train a YOLOR model. To address this challenge, two augmentation

Fig. 1 UGA Road Test Van

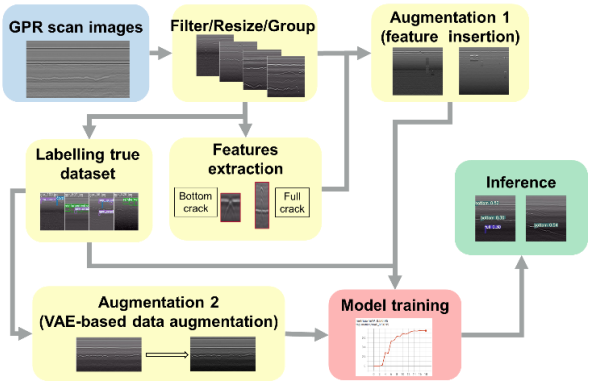

Fig. 2 Data pipeline, model training and inference

methods are proposed. The first method involves generating synthetic images by inserting target features into the images without any target features. The second method uses the available featured images to generate new feature images.

The resulting synthetic images are used for training the YOLOR model. The process is illustrated in Fig. 2.

Particularly, the collected data is divided into two groups: one with target features (referred to as featured images) and the other without target features (referred to unfeatured images). The images with target features are manually labelled with respect to the format required by YOLOR training. The abundant unfeatured images are used as background images for creating synthetic data by inserting extracted target feature patches (referred to as Augmentation 1 in Fig. 2), while the featured images are used to generate new featured images (referred to as Augmentation 2 in Fig. 2)

As shown in Fig. 2, the module (in blue) depicts the GPR image acquisition from scanned road sections. The modules (in yellow) illustrate the formation of the dataset for model training, which includes the use of the two augmentation methods for obtaining synthetic data. The module (in pink) shows the YOLOR model training and testing while the module (in green) indicates the use of trained model for inference.

3.1 GPR dataset

A total of 6,000 images were extracted from GPR scan recordings, followed by a screening process to extract 500

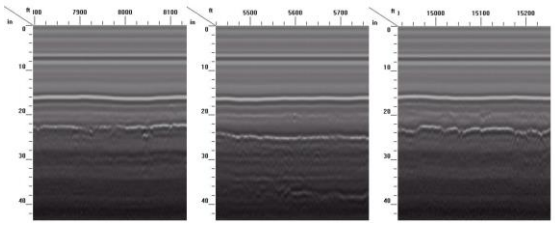

Fig. 3 Extracted GPR images

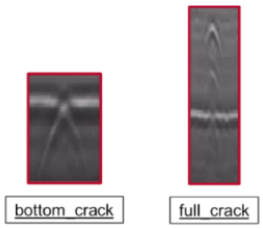

Fig. 4 GPR features to be extracted

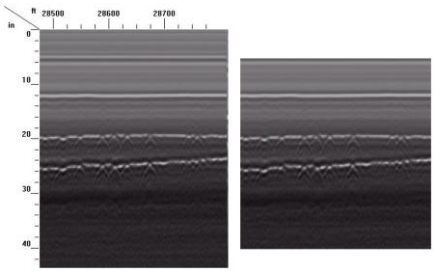

Fig. 5 Image cropped to focus on pavement layers only

images with noticeable features, which are manually labelled. Fig. 3 shows examples of extracted images.

As shown in Fig. 3, irregularities in the GPR images have unique features and are indicative of internal cracks. The examples of enlarge feature patches representing two dominant crack types (i.e., bottom cracks and full cracks) are shown in Fig. 4.

These distinctive features in GPR scans that indicate the presence of cracks in pavement inspired us to utilize deep learning-based object detection algorithms for their identification.

The detection of cracks in GPR images relies on the analysis of variations in electromagnetic wave propagation velocity across each pavement layer. The presence of cracks and voids in the pavement material results in inhomogeneity, which is revealed through a characteristic hyperbolic signature or reflection pattern in the GPR image. By examining the amplitude and frequency of the reflected electromagnetic wave, it is possible to estimate the dimensions of the crack, including its depth, length, and width.

For proper detection of these target features, image cropping is necessary so that the algorithm can focus on the region of interest, i.e., the pavement layers only. Fig. 5 shows both the raw image and the cropped images.

After the images are cropped to the region of interest, they are annotated with the target features. As a result, a total of 500 images were annotated and the captured target features are summarized in Table 1.

Table 1 GPR Scan Image Annotation

Class	Label	# of images	# of labels
bottom_crack	0	360	1929
full_crack	1	274	329

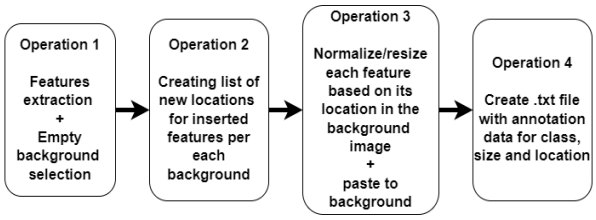

Fig. 6 The process of generating synthetic data by feature insertion

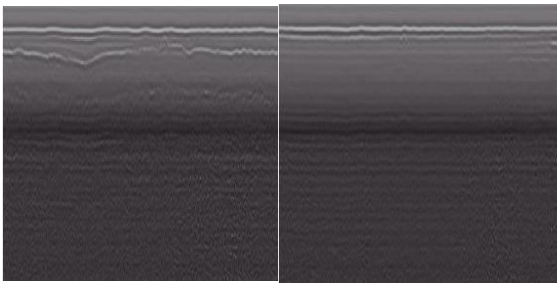

Fig. 7 Empty background with no features for synthetic data creation

The labels presented in the table are based solely on the presence or absence of a bottom crack or a full crack and where they are located in each image. The images contain both types of cracks.

While the utilization of online labeling tools enabled the authors to streamline the labeling process and improve efficiency, the manual labeling process was crucial in ensuring the accuracy of the dataset used for our study.

Since the number of annotated images is quite limited for model training, synthetic data are generated to augment this labeled dataset for training the YOLOR model. Two data augmentation methods are used and discussed in the following subsections.

3.2 Data augmentation with feature insertion

In the context of object detection, an easy way to generate synthetic data with labels is through feature insertion. Four sequential operations (see Fig. 6) are followed to generate synthetic images by feature insertion.

Fig. 7 shows some examples of object-free images, which are used as backgrounds for superimposing target features.

The target feature patches, as illustrated in Fig. 4, are superimposed to the background images at proper locations. For generating realistic featured images, the locations of target features are required to be below the asphalt layer line and they should not overlap with each other.

A series of transformations are applied by considering the pixel values of the valid insertion locations to ensure

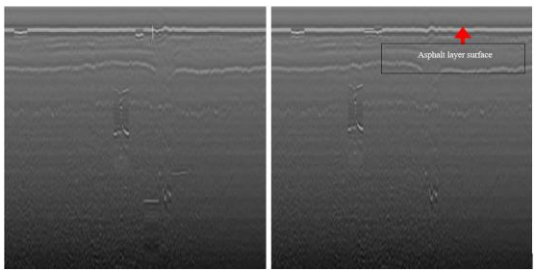

Fig. 8 Example synthetic images generated by our algorithm

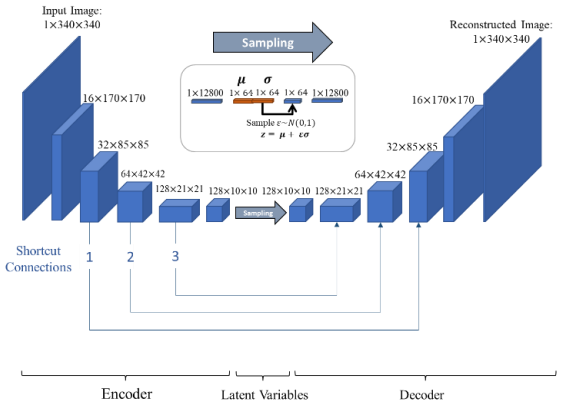

Fig. 9 Variational autoencoder with shortcut connections

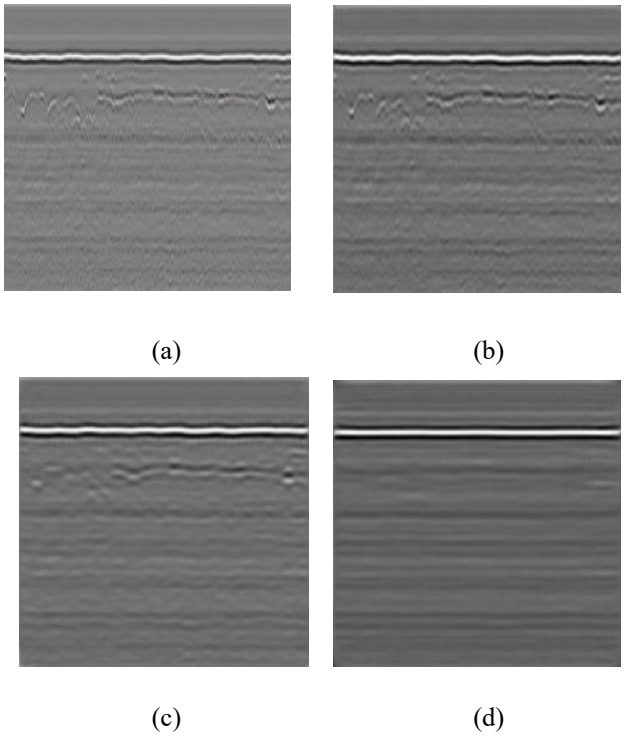

Fig. 10 Comparison of (a) original image, (b) generated image with shortcut connections 1-3 (see Fig. 9), and (c) generated image with shortcut connections 2 and 3, and (d) generated image out shortcut connection 3

realistic looking of the synthetic images. These transformations include resizing, scaling, normalization, and blending. Some exemplar synthetic images generated from this process are shown in Fig. 8.

Since the inserted locations and feature types are known, the labels for these inserted features can be generated automatically, which greatly minimizes the annotation effort. However, depending on the insertion locations, the applied transformations may introduce some artifacts along the boundaries of inserted feature patches. Additionally, the resultant synthetic images may lack variation in target features. Due to these drawbacks, we also employed another Variational Auto-Encoders (VAE) based augmentation method to generate more natural looking featured images, which is discussed subsequently.

3.3 Data augmentation with generative models

An approach for dataset augmentation is to use generative models, such as Generative Adversarial Networks (GAN) (Goodfellow *et al.* 2014), and VAE (Kingma and Welling 2013). However, since there are not enough featured images to train a generative model at the first place, we use VAE with a compromised design that allows the low-level feature information to be utilized to generate new images. The adopted VAE architecture is shown in Fig. 9.

As shown in Fig. 9, corresponding feature blocks between the encoder and decoder are connected through shortcut connections. These shortcut connections help to pass the learned low-level target features to the decoder to generate fine-grained images. Because of the shortcut connections, the latent z (the bottleneck layer) only captures slimited information. As a result, the generated images are very similar to the input images with some textural differences.

Fig. 10 shows examples of generated images by the VAE with different combinations of the skip connections.

Although these VAE-generated images lack feature diversity, our experiment shows that the inclusion of such augmented data results in further improved performance of the model.

With both augmentation methods, a total of 9,174 GPR images is obtained. This dataset is partitioned for training, validation, and testing, as shown in Table 2.

It should be pointed out that the training dataset includes only synthetic images while the validation dataset has both synthetic and real images. The test dataset includes only real images.

Table 2 Data Partition for Model Training, Validation and Testing

Dataset	# of images	Comment
Train	7,674	All synthetic images
Validation	1,000	100 real featured images and 900 synthetic images
Test	500	All real images (400 featured images + 100 background images)
Total	9,174	The entire dataset includes a total of 23,272 target features

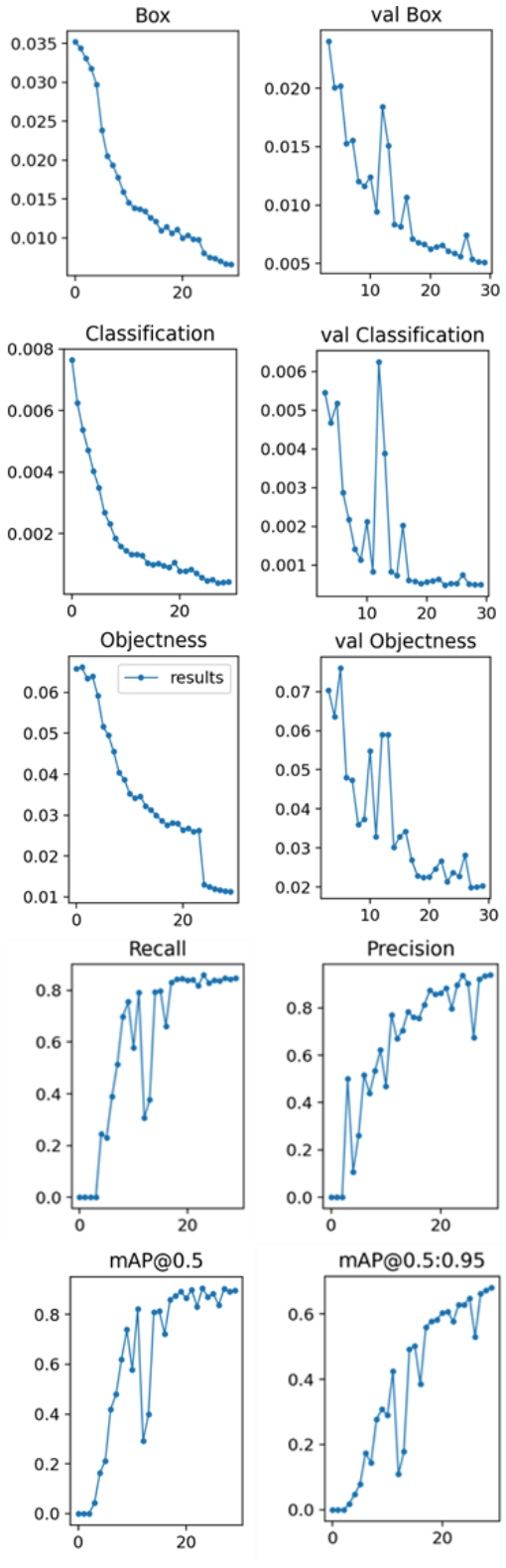

Fig. 11 Training progress of the YOLOR model

4. Experiments

The YOLOR-P6 model is adopted. We leverage transfer learning using pretrained weights with the COCO data. The

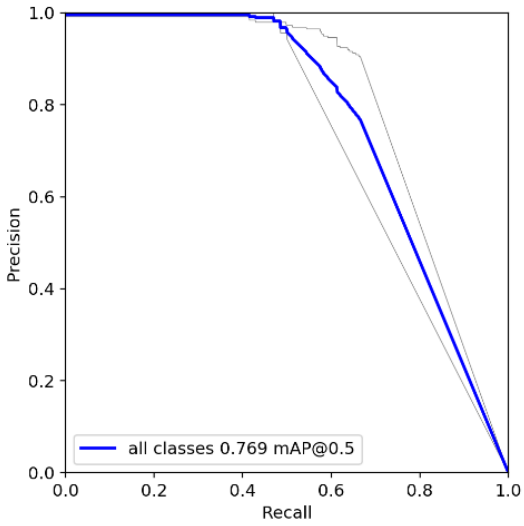

Fig. 12 Precision-Recall curve

model training was conducted using a workstation with Intel® Xeon® CPU @ 2.30GHz, 13 GB RAM, and NVIDIA Tesla K80 GPU. The same YOLOR loss function was used. The classification head was modified to reflect two crack classes. We used Adam for training with a batch size of 8. The initial learning rate was set to 0.001. As the commonly adopted metric for objection detection, Average Precision (AP) at IOU = 0.5 is reported. AP is computed based on the precision and recall curve. Precision and recall are defined by Eqs. (1) and (2).

$$\text{Precision} = TP / (FP + TP) \tag{1}$$

$$\text{Recall} = TP / (FN + TP) \tag{2}$$

where, TP, FP, and FN refer to true positive, false positive, and false negative. The training progress are depicted in Fig. 11. The training converges with a validation AP of 0.896.

To truly evaluate the model performance, the test dataset, which contains only original featured images, is utilized. Fig. 12 shows the precision-recall curve from the test data. As a result, a similar performance is observed with the test data. The Aps@0.5 of 0.769, 0.803 and 0.735 are achieved for all cracks, bottom cracks, and full cracks, respectively.

5. Conclusions

Automated inspection of pavement subsurface conditions allows timely detection of potential structural issues (e.g., bottom-initiated cracks) and enables cost-effective repair and rehabilitation. In this paper, a deep learning based real-time object detection model, YOLOR, is evaluated for detecting subsurface cracks in GPR scan images. The lack of quality target features for model

training is the main obstacle for deploying deep learning-based models. In this study, the team conducted extensive GPR scans along major interstates in the Atlanta metropolitan area as well as local roads in Athens, Georgia.

The retrieved GPR scan data was preprocessed to filter out suspicious sections with target features. The filtered GPR scans were visually checked to verify the target features, followed by annotation. Due to the scarcity of target features, two data augmentation methods (i.e., feature insertion and generation) are implemented. The feature insertion method can quickly increase the dataset without a need for labeling. However, the features in the synthetic images lack variation. On the other hand, the generation method uses a VAE with shortcut connections. The generated images are basically reconstructed images that are very similar to the original images. Nonetheless, leveraging the augmented data from both methods for training has dramatically improved the model performance. The model achieved a test AP of 0.769 for detecting all crack features in the GPR scan images provided the training data contains only synthetic data. This result attests to the utility and feasibility of using the synthetic data for training quality deep learning models for detecting subsurface cracks.

It should be noted that both data augmentation methods implemented in this study have their respective drawbacks. By collecting additional featured images, more sophisticated generative models, such as conditional GAN (Mirza and Osindero 2014) and StyleGANs (Karras *et al.* 2018, 2020, 2021), can be explored to generate more realistic and diverse featured images to further enhance the model performance.

Although transfer learning was adopted by initializing the YOLOR model with pretrained weights with the COCO dataset, the benefits are limited because of the different natures of the images (i.e., GPR scan images versus the natural images in COCO dataset). As more research studies on applying deep learning methods to GPR scan images become available, sharing pretrained models for transfer learning in the same domain would greatly benefit the continued model development effort in this particular area.

It's important to note that the study only focused on identifying two types of subsurface cracks. It would be beneficial to expand the scope of the study to include other types of subsurface features for more comprehensive evaluation of pavement conditions. Particularly, the study could be extended to combine the deep learning-based model with other numerical models, like density estimation and mechanical properties from other field tests, such as the falling weight deflectometer (FWD). This would produce a more complete and accurate assessment of pavement conditions, allowing for better decisions on maintenance and rehabilitation. Furthermore, use of the deep learning model to detect subsurface cracks and other features, along with data from other sources, provides more information about pavement structure and performance. By integrating different methods and data sources, the accuracy and reliability of pavement condition assessment can be greatly improved to inform effective maintenance and rehabilitation strategies.

References

Abdelmawla A. and Kim, S.S. (2020), "Application of ground penetrating radar to estimate subgrade soil density", *Infrastruct.*, **5**(2), 12. https://doi.org/10.3390/infrastructures5020012.

Al-Nuaimy W., Huang, Y., Nakhkash, M., Fang, M.T.C., Nguyen, V.T. and Eriksen, A. (2000), "Automatic detection of buried utilities and solid objects with GPR using neural networks and pattern recognition", *J. Appl. Geophys.*, **43**(2-4), 157-165. https://doi.org/10.1016/S0926-9851(99)00055-5.

Amaghani, D., Mamou, A., Maraveas, C., Roussis, P., Siorikis, V., Skentou, A. and Asteris, P. (2021). "Predicting the unconfined compressive strength of granite using only two non-destructive test indexes", *Geomech. Eng.*, **25**(4), 317-330. https://doi.org/10.12989/gae.2021.25.4.317.

Benedetto A. and Pensa, S. (2007), "Indirect diagnosis of pavement structural damages using surface GPR reflection techniques", *J. Appl. Geophys.*, **62**(2), 107-123. https://doi.org/10.1016/j.jappgeo.2006.09.001.

Chen S., Wang, H., Xu, F. and Jin, Y.Q. (2016), "Target classification using the deep convolutional networks for SAR images", *IEEE T. Geosci. Remote Sens.*, **54**(8), 4806-4817. https://doi.org/10.1109/TGRS.2016.2551720.

Diamanti N., Redman, D. and Giannopoulos, A. (2010), "A study of GPR vertical crack responses in pavement using field data and numerical modelling", *Proceedings of the XIII International Conference on Ground Penetrating Radar*, Castello Carlo V, Lecce, Italy, June.

Ding J., Chen, B., Liu, H. and Huang, M. (2016), "Convolutional neural network with data augmentation for SAR target recognition", *IEEE Geosci. Remote Sens. Lett.*, **13**(3), 364-368. https://doi.org/10.1109/LGRS.2015.2513754.

Gamba P. and Lossani, S. (2000), "Neural detection of pipe signatures in ground penetrating radar images", *IEEE T. Geosci. Remote Sens.*, **38**(2), 790-797. https://doi.org/10.1109/36.842008.

Girshick R., Donahue, J., Darrell, T. and Malik, J. (2014), "Rich feature hierarchies for accurate object detection and semantic segmentation", *Proceedings of the 2014 IEEE Conference on Computer Vision and Pattern Recognition*, Columbus, OH, USA, June.

Goodfellow I.J., Pouget-Abadie, J., Mirza, M., Xu, B., Warde-Farley, D., Ozair, S., Courville, A. and Bengio, Y. (2014), "Generative adversarial networks", *arXiv*:1406.2661.

Karras T., Aittala, M., Hellsten, J., Laine, S., Lehtinen, J. and Aila, T. (2020), "Training generative adversarial networks with limited data", *arXiv*:2006.06676.

Karras T., Aittala, M., Laine, S., Härkönen, E., Hellsten, J., Lehtinen, J. and Aila, T. (2021), "Alias-free generative adversarial networks", *arXiv*:2106.12423

Karras T., Laine, S. and Aila, T. (2018), "A style-based generator architecture for generative adversarial networks.", *arXiv*:1812.04948.

Kingma D.P. and Welling, M. (2013), "Auto-encoding variational bayes", *arXiv preprint arXiv*:13126114.

Kong, S.M., Kim, D.M., Lee, D.Y., Jung, H.S. and Lee, Y.J. (2018), "Field and laboratory assessment of ground subsidence", *Geomech. Eng.*, **16**(3), 285-293. https://doi.org/10.12989/gae.2018.16.3.285.

Krizhevsky, A., Sutskever, I. and Hinton, G.E. (2012), "ImageNet classification with deep convolutional neural networks", *Proc. Advances in Neural Information Processing Systems*, **25**, 1090-1098.

Kwon, S.Y., Yoo, M. and Hong, S. (2020), "Earthquake risk assessment of underground railway station by fragility analysis based on numerical simulation", *Geomech. Eng.*, **21**(2), 143-152. https://doi.org/10.12989/gae.2020.21.2.143.

Lee, K.H., Park, J.H., Park, J., Lee, I.M. and Lee, S.W. (2022), "Experimental verification for prediction method of anomaly ahead of tunnel face by using electrical resistivity tomography", *Geomech. Eng.*, **20**(6), 475-484. https://doi.org/10.12989/gae.2020.20.6.475.

Li, J., Gu, J., Huang, Z. and Wen, J. (2019), "Application research of improved YOLO V3 algorithm in PCB electronic component detection.", *Appl. Sci.*, **9**, 3750.

Mirza M. and Osindero, S. (2014), "Conditional generative adversarial nets", *arXiv*:**1411.1784**.

Saarenketo T. and Scullion, T. (2000), "Road evaluation with ground penetrating radar", *J. Appl. Geophys.*, **43**(2-4), 119-138. https://doi.org/10.1016/S0926-9851(99)00052-X.

Shaw, M.R., Millard, S.G., Molyneaux, T.C.K., Taylor, M.J. and Bungey, J.H. (2005), "Location of steel reinforcement in concrete using ground penetrating radar and neural networks", *NDT & E Int.*, **38**(3), 203-212. https://doi.org/10.1016/j.ndteint.2004.06.011.

Sudyka J., Krysiński, L., Zofka, A., Mechowski, T. and Harasim, P. (2018), "Identification of deep-rooted transverse cracks using Ground Penetrating Radar", *IOP Conf. Ser.: Mater. Sci. Eng*., **356**, 012022.

Wang, C.Y., Yeh, I.H. and Liao, H.Y.M. (2021), "You only learn one representation: Unified network for multiple tasks", *arXiv preprint* **arXiv:2105.04206**.